5-1-2004

Preparation of Nanocomposites from Styrene and Modified Graphite Oxides

Fawn Marie Uhl
Marquette University

Charles A. Wilkie
Marquette University, charles.wilkie@marquette.edu

Chemistry Faculty Research and Publications/College of Arts and Sciences

Preparation of Nanocomposites from Styrene and Modified Graphite Oxides

Fawn M. Uhl
Department of Chemistry, Marquette University, P.O. Box 1881, Milwaukee, WI
Charles A. Wilkie
Department of Chemistry, Marquette University, P.O. Box 1881, Milwaukee, WI

Abstract

Graphite oxide was prepared and modified with several ammonium salts and these modified graphite oxides were used to prepare nanocomposites with polystyrene by in situ polymerization of styrene monomer and by melt blending with polystyrene. Nanocomposites were characterized by X-ray diffraction, cone calorimetry, thermogravimetric analysis and the evaluation of mechanical properties. Nanocomposites are formed by in situ polymerization but not by melt blending; the graphite oxide undergoes thermal degradation at the temperature of melt blending so nanocomposite formation would be unlikely. Mechanical properties of the melt blended nanocomposites are improved relative to the virgin polystyrene while those prepared by in situ polymerization are decreased, except in the case of Young's Modulus, where melt blended and in situ polymerized materials show similar results.

Keywords

Graphite oxide, Polystyrene, Nanocomposites, Cone calorimetry

1. Introduction

Research in this, and other laboratories, has focused on the preparation of clay–polymer nanocomposites and the effect nanocomposite formation on the flammability of polymers [1], [2], [3], [4], [5], [6], [7], [8], [9], [10]. It has been shown that these nanocomposites exhibit a reduction in flammability and an increase in mechanical properties, offering a unique opportunity for enhanced fire retardancy of these systems. It has been suggested that the enhancement is due to the layered structure of the clay; an examination of other layered materials may lead to nanocomposites where an enhancement in polymer properties can also be observed.

In this laboratory, in addition to clay systems, graphite–polymer nanocomposites have been studied [11], [12], [13]. It has been shown that potassium graphite can be used to initiate the polymerization of styrene to form graphite–polystyrene nanocomposites [11] and expandable graphite has also been used with various polymers to form nanocomposites [12], [13]. These results demonstrate that graphite can be used as the nano-dimensional material to form nanocomposites and the properties are similar to those obtained using clay.

For both graphite and clay systems, there is an initial intercalation of some material between the layers. In the case of clay this is an organophilic cation, which replaces the sodium counterion that naturally occurs in the clay, while for graphite both potassium and sulfuric acid have been used. Neither of these is organophilic, if one could add something that would make the graphite organophilic, this may improve the interactions between polymer and graphite. Graphite does not undergo any ion exchange process [14], [15], [16], [17], [18] but graphite oxide (GO) will add organophilic ammonium cations between the layers.

The preparation of graphite oxide involves the oxidation of graphite, using an oxidizer in the presence of nitric acid and both stage 1 and stage 2 materials have been formed [19], [20], [21]. Upon formation of graphite oxide the layered structure of graphite is preserved, but the aromatic character is partially lost; the structure contains various amounts of hydroxyl groups, ether groups, double bonds, enol, and ketone groups. The formula that has been suggested for graphite oxide is $C_7O_4H_2$ and it is known to be thermally unstable [20], [21], [22]. Graphite oxide is hydrophilic and readily adsorbs water or other polar liquids; a one-dimensional swelling is observed as the lamellae move apart, similar to clays [20]. The swelling of the graphite oxide allows for intercalation of various compounds such as alkyl ammonium salts and polymers [19], [20], [23], [24], [25], [26], [27], [28], [29]. A variety of surfactants have been intercalated and the exchange capacity is quite large, about 600 meq/100 g of clay [24].

In this study, nanocomposites of polystyrene and organically modified graphite oxide are prepared by both in situ polymerization and melt blending and the resulting material is compared to the graphite and clay nanocomposites of polystyrene.

2. Experimental

2.1. Materials

Most materials were obtained from Aldrich Chemical Company, including polystyrene (PS) (MW, 280,000), graphite (powder, 1–2 μm), styrene and inhibitor remover columns; the inhibitor was removed from monomeric styrene before use. The ammonium salts used were myristyltrimethyl ammonium bromide (C14) (Aldrich), dimethyl hydrogenated tallow benzyl ammonium chloride supplied by Akzo-Nobel as ARQUAD DMHTB-75 (DMHTB), and 4-vinylbenzyl ammonium chloride (VB16) [4]. C14 and DMHTB were used as received and the VB16 salt was prepared by literature procedure [4].

2.2. Instrumentation

A Cahn TG-131 thermoanalyzer was used under a flowing inert atmosphere at a scan rate of 20 °C per minute. Temperatures are reproducible to ±5 °C while the fraction of non-volatile material typically gives error bars of ±2%. Infrared spectra were obtained using a Nicolet Magna infrared 560 spectrometer E.S.P. TGA/FT-IR were performed on a Cahn TG-131 balance interfaced to a Mattson Research Fourier transform infrared spectrometer under inert atmosphere at a scan rate of 20 °C per minute. X-ray diffraction was performed on a

Rigaku Geiger Flex, two-circle powder diffractometer with a Cu tube source (λ=1.54Å) operated a 1 kW. Scans were taken from 2ϑ at 0.70 to 30, step size 0.10, and scan time per step of 20 s using the high resolution mode. Cone calorimetry at 35 kW/m^2 was performed using an Atlas Cone-2 instrument, according to ASTM E 1354-92 at an incident flux of 35 kW/m^2 using a cone shaped heater. Exhaust flow was set at 24 L/s and the spark was continuous until the sample ignited. All samples were run in duplicate, and the average value is reported; typical results from cone calorimetry are reproducible to within about ±10% [30]. Mechanical testing was performed on an Instron testing machine.

2.3. Preparation of graphite oxide—Brodie method [19]

Graphite oxide was prepared by the reaction of graphite, fuming nitric acid, and potassium chlorate. In a typical experiment 15.15 g of graphite was placed in a 2-L flask containing 300 mL of fuming nitric acid cooled in an ice bath. To this was added 119.71 g of potassium chlorate over 1 h, then the reaction mixture was allowed to stir for 6 h. It was then poured into 1500 mL of distilled water, filtered and washed with methanol until a pH greater than 6 was obtained.

2.4. Preparation of modified graphite oxide

Graphite oxide was modified using several ammonium salts, C14, DMHTB, and VB16. The graphite oxide was dispersed in 0.1 M sodium hydroxide by sonication for 30 min and the ammonium salt was dissolved in water, then the ammonium salt solution was poured into the graphite oxide mixture with stirring and a precipitate formed immediately. In a typical experiment, 20 g of graphite oxide was placed in 400 mL of 0.1 M sodium hydroxide and sonicated for 30 min and 8 g of the ammonium salt was dissolved in 400 mL of distilled water. The solutions were mixed and stirred for 30 min and the precipitate was filtered and washed with distilled water.

2.5. Preparation of graphite oxide–polystyrene nanocomposites

Nanocomposites were prepared by two methods, melt blending polystyrene with the graphite oxides or by in situ polymerization of styrene in the presence of the modified graphite oxide; nanocomposites were prepared containing 1, 3, or 5% graphite oxide or modified graphite oxide. In a typical example, 50 g of polystyrene was melt blended with the appropriate amount of graphite oxide/modified graphite oxide at 230 °C for 10 min in a Brabender Plasticorder, then annealed overnight at 120 °C. In the case of the in situ polymerized samples, typically 50 g of styrene monomer was placed in a beaker with appropriate amount of graphite oxide or modified graphite oxide, and 0.2% initiator, AIBN. This mixture was sonicated for 20 min then heated with stirring until a viscous solution formed. The beaker containing this viscous solution was then transferred to an oven at 80 °C and maintained for 48 h under nitrogen; finally vacuum was applied to remove unreacted monomer and the polymer was scrapped out from the beaker.

3. Results and discussion

Graphite oxide has been prepared and organically modified using three different surfactants, the structures of which are shown in Fig. 1. These surfactants have been chosen based upon previous nanocomposite work using clays; VB16 gives exfoliated polystyrene–clay nanocomposites under in situ polymerization conditions while the other two surfactants are not expected to give exfoliation but rather intercalation. X-ray diffraction (XRD) is used to evaluate the *d*-spacing in these materials and cone calorimetry, rather than the more common transmission electron microscopy, is used to evaluate the type of dispersion, nano or micro, that has been achieved.
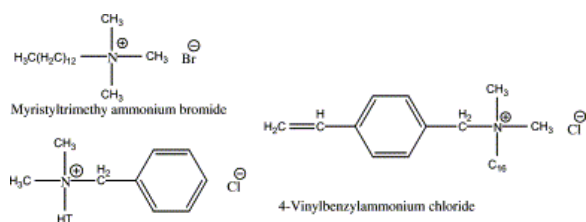
Fig. 1. Structures of ammonium salts.

3.1. X-ray diffraction (XRD) of graphite oxides

The *d*-spacing observed is consistent with that reported in literature; a 2ϑ peak at 13.2° is assigned to the d_{001} peak for graphite oxide [24], [25], [26]. This graphite oxide can undergo an ion exchange process with ammonium salts, forming the corresponding modified graphite oxide, resulting in an increase in the *d*-spacing, see Table 1 and Fig. 2. In the infrared spectrum, peaks attributable to graphite oxide (GO) are observed at 3452 cm^{-1}, OH stretch, 1721 cm^{-1} and 1608 cm^{-1}, C☐C stretch, and 1373 cm^{-1} and 1055 cm^{-1}, C–O stretch. In the spectra of the modified graphite oxides (GO-C14, GO-DMHTB, GO-VB16), peaks characteristic of graphite oxide and new peaks at 2919 cm^{-1}, 2852 cm^{-1} and 1470 cm^{-1}, all attributable to C–H stretch and bend of the alkyl chain on the ammonium cation, indicate that the ammonium ion has been incorporated into the graphite oxide.

Table 1. XRD data for GO and modified GOs

Sample	2ϑ Peaks observed	*d*-spacing (Å)[a]
GO	13.2 (d_{001})	6.7
GO-C14	3.4 (d_{001}), 9.6 (d_{002}), 20.9 (d_{003})	28.7
GO-DMHTB	9.1 (d_{001}), 13.4 (d_{002})	9.7
GO-VB16	2.7 (d_{001}), 9.8 (d_{002}), 13.4 (d_{003})	32.7

[a]Based on reported *d*-spacing of graphite oxide as being the d_{001}.
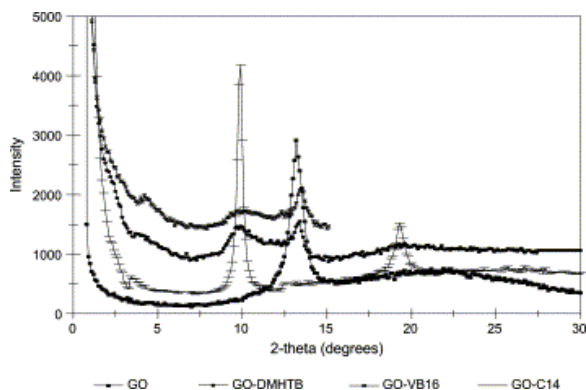
Fig. 2. XRD of GO and its modified salts.

Once the modified graphite oxides were prepared they can be reacted with styrene monomer by in situ polymerization or melt blended with polystyrene to form nanocomposites; Table 2 lists the XRD data for the resulting materials. The absence of a peak in the XRD may be attributable either to the formation of an exfoliated structure or to disorder within the graphite and an additional technique is required to identify the actual situation. For in situ polymerized styrene, no peaks are observed at 1% for all three modified graphite oxides and no peak is observed for two of the three modified graphite oxides at 3% loading; at 5% loading XRD peaks are clearly seen and, since the *d*-spacing has increased from that in the GO, intercalation is indicated. Similar results are observed for the melt blended system; the presence of a peak at a lower value of 2ϑ gives an initial indication that an intercalated system has been produced. Thus one may begin to identify the types of nanocomposites that have been produced based on the XRD data.

Table 2. XRD data for nanocomposites prepared by in situ polymerization of styrene and melt blending with PS in the presence of graphite oxide and modified graphite oxide

Sample	1%, 2ϑ	3%, 2ϑ	5%, 2ϑ
GO/PS, in situ	15.6 (d_{002})	15.6 (d_{002})	15.6 (d_{002})
GO-C14/PS, in situ	No peak	8.6 (d_{002})	8.8 (d_{002}), 17.9 (d_{003})
GO-10A/PS, in situ	No peak	No peak	2.3 (d_{001})
GO-VB16/PS, in situ	No peak	No peak	14.7 (d_{004})
GO/PS, melt blended	15.6 (d_{002})	15.6 (d_{002})	15.6 (d_{002})
GO-C14/PS, melt blended	1.1 (d_{001}), 1.7 (d_{002}), 10.9 (d_{003})	10.8 (d_{003})	10.9 (d_{003})
GO-10A/PS, melt blended	No peak	11.1 (d_{002})	1.2 (d_{001}), 11.1 (d_{002})
GO-VB16/PS, melt blended	No peak	No peak	No peak

3.2. Cone calorimetry

The parameters that may be evaluated from cone calorimetry include the heat release rate, times to ignition and peak heat release rate, specific extinction area (SEA), a measure of smoke, and the mass loss rate. If any one cone parameter is given special attention, it is the rate of heat release and its peak value, PHRR, because this gives information on the type of fire hazard that may be encountered. It has also been shown that the formation of a nanocomposite gives rise to the maximum reduction in PHRR while a microcomposite, also known as an immiscible nanocomposite, gives minimal reduction, in the range of 10–15%, in PHRR [31], [32]. This piece of data is extremely useful both for the fire scientist and for the individual interested in evaluating the type of nanocomposite that has been produced. The time to ignition tells how easy it is for the material to ignite, it is ordinarily found that nanocomposites are more easily ignited than is the virgin polymer. The time to PHRR gives an indication of the shape of the heat release curve; ideally one would like to increase this time so as to reduce the fire hazard. The specific extinction area is a measure of the amount of smoke that is evolved during the combustion; a reduction in the value would be good but this is usually not seen with nanocomposites. Finally the mass loss rate tells if the combustion process has been changed due to the presence of the additive.

It has been shown in work from this laboratory [33], [34], [35], [36] that cone calorimetry may be a more reliable indicator of dispersion than is transmission electron microscopy, TEM. TEM examines only a very small piece of the sample, which may or may not be representative of the whole, while cone calorimetry looks at the entire sample. There is not yet a theory to explain the correlation between dispersion and the reduction in PHRR. At this time all that has been stated is that, if the reduction is comparable to the best value that has been observed for a particular polymer, then the nano-phase material is well-dispersed throughout the polymer. If the reduction is significantly less than the maximum reduction, this indicates the presence of a substantial immiscible component. Good agreement with this assertion has been shown for PS nanocomposites formed using a polybutadiene-modified clay. When melt blending was used to form the nanocomposite, TEM showed that the material was immiscible and the reduction in PHRR was 7%. When bulk polymerization was used, TEM showed that good nano-dispersion was obtained and there was a 42% reduction in PHRR [35]. In related work, this same clay was melt blended with several other polymers and TEM in all cases showed that immiscible materials were formed; the reduction in PHRR was minimal for all polymers [36].

Cone calorimetric results are shown in Table 3, Table 4 and Fig. 3, Fig. 4 for in situ polymerized and melt blended nanocomposites, respectively. For the in situ polymerization, the reduction in PHRR ranges from 27 to 54%; the reduction in PHRR usually increases as the fraction of GO increases. It is surprising to observe that GO as well as modified GOs give qualitatively similar reductions in PHRR. Since graphite oxide has not been organically modified, one might suspect that a nanocomposite could not form. The XRD results show that expansion of the d-spacing has occurred and the cone results suggest that some nanocomposite formation does occur. Perhaps the presence of the functional groups on the graphite oxide provides sufficient organic modification to permit the incorporation of polymer between the layers. It must be remembered that the only

assertion that can be made is that, if the reduction is equivalent to the maximum reduction which has been previously seen, then good nano-dispersion has been achieved. We must conclude from the cone calorimetry data that there are both intercalated/exfoliated and immiscible components in these graphite oxide–styrene nanocomposites.

Table 3. Cone calorimetry results for in situ polymerized GO–styrene nanocomposites

Sample	% Graphite oxide	PHRR (kW/m^2) (reduction)	Time to ignition (s)	SEA (m^2/kg)	Mass loss rate (g/sm^2)
PS—in situ polymerization	0	1439 ± 98	47 ± 2	1280 ± 128	17 ± 1
GO					
	1	950 ± 38 (34)	27 ± 3	1015 ± 31	18 ± 1
	3	916 ± 31 (36)	13 ± 1	956 ± 51	16 ± 1
	5	797 ± 24 (45)	19 ± 2	1023 ± 19	15 ± 1
GO-10A					
	1	967 ± 82 (33)	10 ± 1	1285 ± 107	16 ± 2
	3	805 ± 32 (44)	11 ± 3	1204 ± 78	16 ± 1
	5	707 ± 37 (51)	9 ± 3	1261 ± 45	16 ± 1
GO-C14					
	1	1054 ± 22 (27)	17 ± 2	1144 ± 57	16 ± 1
	3	827 ± 43 (43)	19 ± 5	1297 ± 78	17 ± 1
	5	665 ± 47 (54)	12 ± 2	1297 ± 78	15 ± 1
GO-VB16					
	1	838 ± 50 (42)	10 ± 1	1258 ± 87	16 ± 2
	3	732 ± 37 (49)	20 ± 6	1158 ± 72	17 ± 2
	5	689 ± 51 (52)	14 ± 2	1239 ± 74	17 ± 1

Table 4. Cone calorimetry results for melt blended GO–styrene nanocomposites using commercial PS

Sample	% Graphite oxide	PHRR (kW/m^2) (reduction)	Time to ignition (s)	SEA (m^2/kg)	Mass loss rate (g/sm^2)
PS—melt blended	0	1180 ± 22	55 ± 1	938 ± 52	18 ± 1
GO					
	1	986 ± 27 (16)	33 ± 1	987 ± 85	15 ± 1
	3	917 ± 21 (22)	23 ± 1	972 ± 39	16 ± 1
	5	855 ± 18 (27)	18 ± 1	995 ± 33	16 ± 1
GO-10A					
	1	1166 ± 49 (1)	42 ± 2	958 ± 7	13 ± 1
	3	1052 ± 49 (11)	39 ± 3	892 ± 77	15 ± 1
	5	1042 ± 42 (12)	34 ± 2	1097 ± 91	14 ± 1
GO-C14					
	1	1109 ± 19 (6)	43 ± 3	1188 ± 88	17 ± 1
	3	999 ± 2 (15)	31 ± 1	1268 ± 70	17 ± 1
	5	910 ± 24 (23)	27 ± 1	1371 ± 70	19 ± 1
GO-VB16					
	1	983 ± 108 (17)	41 ± 1	1257 ± 87	16 ± 2
	3	910 ± 33 (23)	35 ± 2	1139 ± 14	18 ± 2
	5	939 ± 21 (20)	33 ± 4	1142 ± 20	18 ± 1
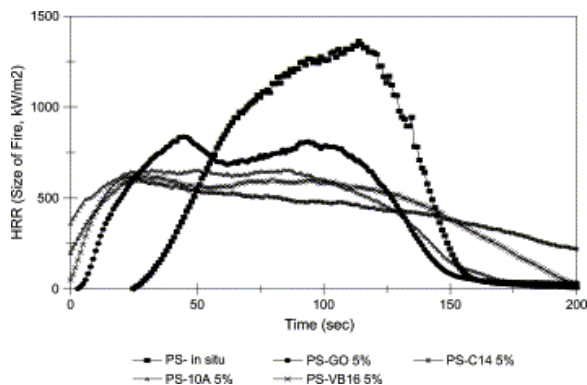
Fig. 3. Heat release curves for in situ polymerized PS–graphite oxide nanocomposites.
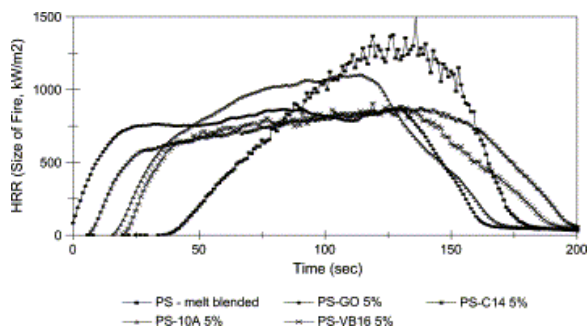
Fig. 4. Heat release rate curves for melt blended PS–graphite oxide nanocomposites.

The time to ignition is drastically decreased for the graphite oxide nanocomposites compared to virgin polystyrene; a reduction in time to ignition is invariably observed for nanocomposites; these values are less than those seen for the PS nanocomposites that were prepared using KC_8 as the initiator [11].

The reduction in PHRR for the melt blended nanocomposites is much smaller than observed for in situ polymerized material; the error bars on cone parameters are ±10% and thus a change in the range of 15–20% is minimally a change in the PHRR. One may conclude that nanocomposite formation does not occur with the melt blended systems. All of the other cone parameters, time to ignition, smoke and mass loss rate, are similar for both melt blended and in situ polymerized material.

The combination of cone calorimetry and X-ray diffraction indicates that exfoliated nanocomposites are produced for in situ polymerization at low clay loading, 1–3%, and an intercalated material is obtained when 5% clay is present. A similar result, exfoliation at low amounts of the nano-phase material and intercalation at higher amounts, has also been observed for polyamide-6-clay nanocomposites [37]. For melt blended systems, the *d*-spacing does not change very much for any system and, in those cases where no peak is detected, one must invoke disorder in the graphite rather than the formation of an exfoliated system. This is completely reasonable since it is known that graphite oxide will undergo thermal degradation above 180 °C to give graphite and virgin graphite does not give a nanocomposite upon blending with polystyrene.

3.3. Thermogravimetric analysis

The thermogravimetric analysis data for the nanocomposites prepared by in situ polymerization and melt blending are shown in Table 5, Table 6, respectively. The data that are reported include the onset temperature of the degradation, as measured by the temperature at which 10% of the sample is lost, $T_{10\%}$, the mid-point of the degradation T_{max} and the fraction of non-volatile residue which remains at 600 °C, char. In the case of in situ polymerized nanocomposites the onset temperatures and the mid-point temperatures of the degradation are similar for all of the modified graphite oxides and are not very different from that of polystyrene. It is surprising to note that the temperatures increase for the graphite oxide–PS system. For the

melt blended materials, where no nanocomposite formation is expected, there is approximately the same increase in temperature as is seen for the graphite oxide–PS in situ polymerized material. These TGA results are comparable to those obtained for other graphite–PS nanocomposites but they are quite different from what is seen for polystyrene–clay systems. Further work is required to understand these variations.

Table 5. Thermogravimetric data for in situ polymerized GO–styrene nanocomposites

Sample	$T_{10\%}$ (°C)	T_{max} (°C)	Char (%)
PS—in situ	373 ± 1	419 ± 1	1 ± 1
GO-VB16/PS			
1%	369 ± 4	417 ± 0	4 ± 1
3%	387 ± 6	421 ± 4	5 ± 1
5%	383 ± 1	418 ± 3	7 ± 1
GO-10A/PS			
1%	381 ± 2	420 ± 3	4 ± 2
3%	375 ± 5	423 ± 5	6 ± 2
5%	363 ± 6	426 ± 1	9 ± 1
GO-C14/PS			
1%	362 ± 5	419 ± 3	2 ± 1
3%	375 ± 4	424 ± 1	8 ± 1
5%	341 ± 5	422 ± 5	5 ± 2
GO/PS			
1%	405 ± 4	451 ± 6	2 ± 1
3%	403 ± 4	448 ± 4	7 ± 1
5%	401 ± 1	445 ± 4	11 ± 1

Table 6. Thermogravimetric data for melt blended GO–styrene nanocomposites

Sample	$T_{10\%}$ (°C)	T_{max} (°C)	Char (%)
PS—melt blended	351	418	0
GO-VB16/PS			
1%	404 ± 2	450 ± 0	1 ± 1
3%	403 ± 1	446 ± 3	3 ± 1
5%	404 ± 1	451 ± 2	3 ± 1
GO-10A/PS			
1%	401 ± 1	448 ± 1	1 ± 1
3%	402 ± 7	448 ± 1	2 ± 1
5%	411 ± 1	450 ± 0	3 ± 1
GO-C14/PS			
1%	395 ± 2	442 ± 4	1 ± 1
3%	402 ± 1	449 ± 4	2 ± 1
5%	398 ± 5	449 ± 5	2 ± 1
GO/PS			
1%	381 ± 3	439 ± 5	3 ± 1
3%	381 ± 3	437 ± 4	3 ± 1
5%	377 ± 0	437 ± 0	3 ± 1

3.4. TGA/FT-IR studies

3.4.1. Graphite oxide (GO)

It has been shown that graphite oxide undergoes degradation around 180 °C; releasing carbon monoxide, carbon dioxide, and water [21]. Fig. 5 shows the FT-IR spectrum for graphite oxide degradation products at 210 °C and 590 °C; the spectra between the two temperatures does not significantly change. From Fig. 5 peaks at 3585 cm^{-1} (OH symmetric stretch), 3740 cm^{-1} (OH asymmetric stretch), and 1644 cm^{-1} (HOH scissoring) are observed, indicating the release of water. The peak at 2360 cm^{-1} is typical for carbon dioxide while the peaks at 2170 and 2136 cm^{-1} are representative of carbon monoxide loss.
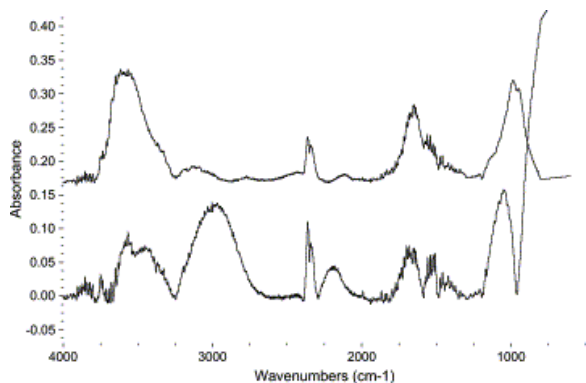
Fig. 5. FT-IR spectra of graphite oxide degradation products, top, 590 °C and bottom, 210 °C.

3.4.2. Modified GOs

The TGA/FT-IR spectra, shown in Fig. 6, for the modified graphite oxides are similar to that of un-modified graphite oxide; the major peaks observed are those for water, carbon monoxide, and carbon dioxide.
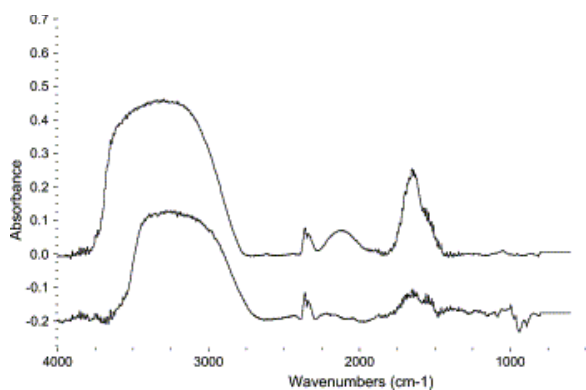
Fig. 6. FT-IR spectrum of a modified graphite oxide (GO-VB16). Top spectrum is at 580 °C and bottom is at 190 °C.

3.4.3. In situ polymerized nanocomposites

Fig. 7 shows the FT-IR spectrum of the degradation products for an in situ polymerized nanocomposite. The degradation of the graphite oxide occurs at the lowest temperature, as seen by peaks due to water, CO, and CO_2. The second step is the degradation of the ammonium salt and peaks due to aliphatic C–H stretching and bending are observed. Finally above 435 °C the presence of aromatic C–H stretching frequency signifies loss of styrene.
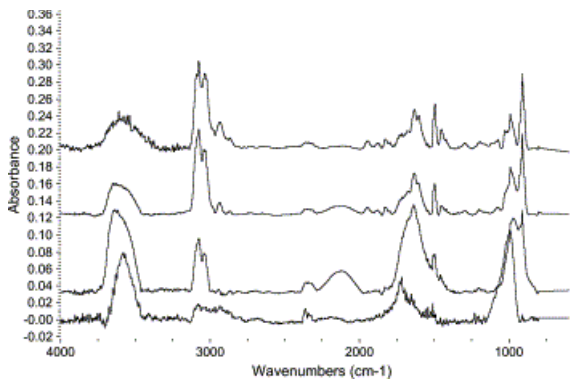
Fig. 7. FT-IR spectra of in situ polymerized composite (GO-VB16/PS) at 310 °C (bottom, 5% mass loss), 415 °C (second, 10% mass loss), 435 °C (third, 25% loss), and 460 °C (top, 60% mass loss).

3.4.4. Melt blended nanocomposites

The degradation process of the melt blended nanocomposites, Fig. 8, looks slightly different from that of the in situ polymerized nanocomposites; the 5% weight loss for the melt blended nanocomposites occurs ~80 °C higher than for the in situ polymerized material. The spectra for the melt blended show peaks attributable to C–H stretching at low mass loss, while the in situ polymerized material shows peaks typical of the degradation of GO. This suggests that the graphite oxide (GO) structure in the melt blended nanocomposites may have been destroyed upon processing and the mass which is lost is due to the degradation of the polymer. As the temperature increases, the volatiles are typical of polystyrene.
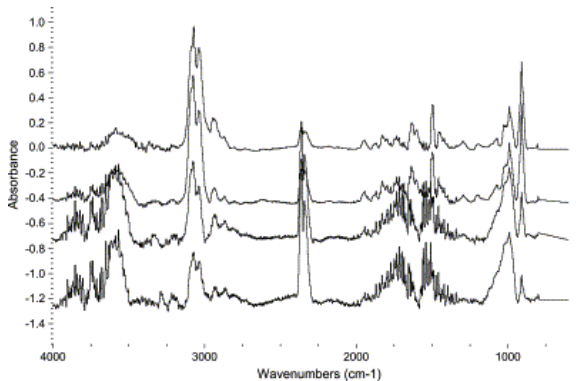
Fig. 8. FT-IR spectra of melt blended composites (GO-VB16/PS); bottom 390 °C (5% mass loss), second 410 °C (10% mass loss), third 430 °C (25% loss), and top 440 °C (60% mass loss).

3.4.5. Mechanical properties

In general the mechanical properties of the in situ polymerized and melt blended nanocomposites are not severely impacted by presence of graphite oxide. The tensile strength at break is shown in Fig. 9 for in situ polymerized and Fig. 10 for melt blended composites. In situ polymerized nanocomposites show a decrease in tensile strength as the amount of graphite oxide is increased. The non-modified graphite oxide exhibits the worst mechanical properties with a decrease in tensile strength of 90% at 5% loading; this is consistent with the brittleness of the graphite oxide–PS samples prepared for mechanical properties. Tensile strength for the melt blended nanocomposites is higher or the same in most cases with the GO-VB16 nanocomposites exhibiting a decrease in tensile strength.
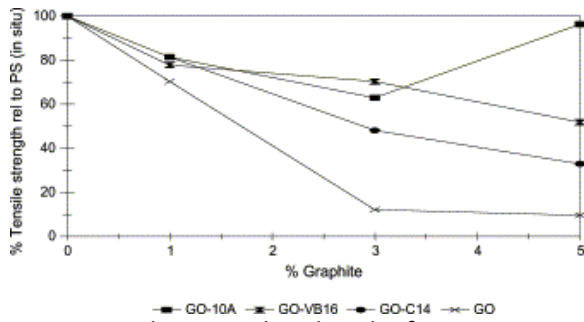
Fig. 9. Tensile strength at break of in situ GO–styrene nanocomposites.
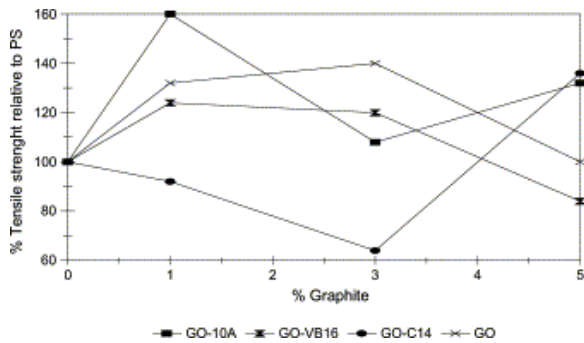
Fig. 10. Tensile strength at break for melt blended GO–styrene nanocomposites.

There is a slight decrease in percent elongation for the in situ polymerized material, but an increase is seen for melt blended materials, Fig. 11, Fig. 12, respectively.
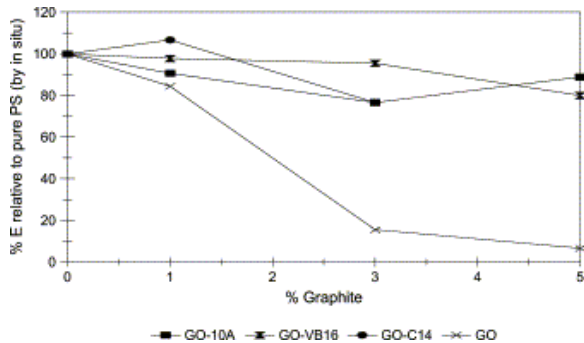
Fig. 11. % Elongation for in situ GO–styrene nanocomposites.
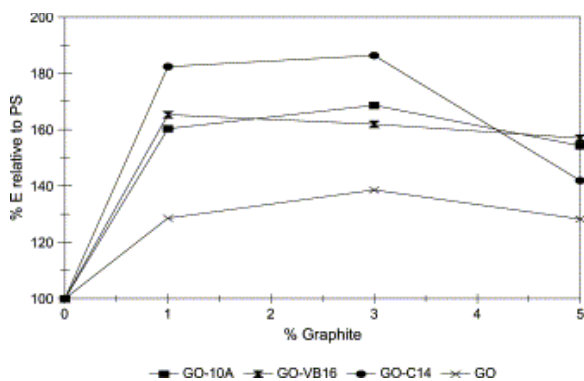
Fig. 12. % Elongation for melt blended GO–styrene nanocomposites.

Table 7 shows the Young's Modulus data for both the in situ and melt blended nanocomposites. The melt blended composites appear to have a slightly higher Young's Modulus compared to the in situ polymerized nanocomposites. In both cases the Young's Modulus of the nanocomposites is similar to that of the pure polystyrene. There does appear to be a decrease as the amount of graphite oxide is increased. In general the

mechanical properties of the melt blended nanocomposites appear to be better than those of the in situ polymerized composites. Based on cone calorimetry results and the mechanical property results, one can conclude that because there is no reduction in PHRR for these nanocomposites they are acting as filler, which is consistent with the results for mechanical properties, where no significant change in all mechanical properties is observed. The results for the in situ polymerized nanocomposites are consistent with other graphite–polystyrene nanocomposites prepared in this laboratory, where a decrease in PHRR is observed along with a decrease in mechanical properties.

Table 7. Young's Modulus data for GO–styrene nanocomposites

In situ sample	% Graphite oxide	Young's Modulus (Gpa) in situ	Young's Modulus (Gpa) melt blended
PS	0	2.5	3
GO-10A			
	1	2	3.7
	3	2.4	3.8
	5	2.8	2.7
GO-VB16			
	1	3.1	2.4
	3	2.1	2.5
	5	1.7	1.9
GO-C14			
	1	3.3	2.6
	3	3.6	2.4
	5	2.4	2.9
GO			
	1	2.2	2.8
	3	[a]	2.6
	5	[a]	1.6

[a]Data could not be obtained.

4. Conclusions

X-ray diffraction suggests that nanocomposites have been formed by in situ polymerization and melt blending of various graphite oxides with polystyrene. Graphite oxide nanocomposites prepared by in situ polymerization exhibit a significant reduction in peak heat release rate comparable to that of clay–polystyrene nanocomposites. The melt blended nanocomposites show a decrease but not significant. This suggests that nanocomposites are actually formed under bulk polymerization conditions but not by melt blending. These results confirm that has been earlier asserted, that one can evaluate dispersion by cone calorimetry.

Acknowledgements

References

[1] J.W. Cho, D.R. Paul. *Polymer*, 42 (2001), pp. 1083-1094
[2] A.C. Balazs, C. Singh, E. Zhulina, Y. Lyatskaya. *Acc Chem Res*, 32 (1999), pp. 651-657
[3] J. Zhu, F.M. Uhl, A.B. Morgan, C.A. Wilkie. *Chem Mater*, 13 (2001), pp. 4649-4654
[4] J. Zhu, A.B. Morgan, F.J. Lamelas, C.A. Wilkie. *Chem Mater*, 13 (2001), pp. 3774-3780
[5] D. Wang, D. Parlow, Q. Yao, C.A. Wilkie. *J Vinyl Add Tech*, 7 (2001), pp. 203-213

[6] J. Zhu, F. Uhl, C.A. Wilkie. G.L. Nelson, C.A. Wilkie (Eds.), Fire and polymers materials and solutions for hazard prevention. *ACS Symposium series 797*, Oxford University Press (2001), pp. 24-33

[7] A.B. Morgan, T. Kashiwagi, R.H. Harris, J.R. Campbell, K. Shibayama, K. Iwasa, *et al..* G.L. Nelson, C.A. Wilkie (Eds.), *Fire and polymers materials and solutions for hazard prevention*, Oxford University Press (2001), pp. 9-23

[8] J. Zhu, C.A. Wilkie. *Polym Int*, 49 (2000), pp. 1158-1163

[9] J.W. Gilman, C.L. Jackson, A.B. Morgan, R. Harris. *Chem Mater*, 12 (2000), pp. 1866-1873

[10] X. Fu, S. Qutubuddin. *Polymer*, 42 (2001), pp. 807-813

[11] F.M. Uhl, C.A. Wilkie. *Polym Degrad Stab*, 76 (2002), pp. 111-122

[12] Uhl FM, Yao Q, Wilkie CA. *Expandable graphite/polyamide-6 nanocomposites*, in preparation.

[13] Uhl FM, Yao Q, Wilkie CA. *Effect of expandable graphite on styrene and copolymers in composite formation*, in preparation.

[14] J.M. Lalancette, R. Roussel. *Can J Chem*, 54 (1976), pp. 2110-2115

[15] J.M. Lalancette, R. Rollin, P. Dumas. *Can J Chem*, 50 (1972), pp. 3058-3062

[16] G.R. Hennig. *Prog Inorg Chem*, 1 (1959), pp. 125-133

[17] W. Rudorff. *Adv Inorg Radiochem*, 1 (1959), pp. 223-266

[18] H. Selig, L.B. Ebert. *Adv Inorg Radiochem*, 23 (1980), pp. 289-327

[19] T. Nakajim, M. Yoshiaki. *Carbon*, 32 (1994), pp. 469-475

[20] I. Dekany, R. Kruger-Grasser, A. Weiss. *Colloid Polym Sci*, 276 (1998), pp. 570-576

[21] A. Lerf, H. He, M. Forster, J. Klinowski. *J Phys Chem B*, 102 (1998), pp. 4477-4482

[22] H. He, T. Riedl, A. Lerf, J. Klinowski. *J Phys Chem*, 100 (1996), pp. 19954-19958

[23] H.N. Patrick, G.G. Warr, S. Manne, I.A. Aksay. *Langmuir*, 13 (1997), pp. 4339-4356

[24] Y. Matsuo, T. Niwa, Y. Sugie. *Carbon*, 37 (1999), pp. 897-901

[25] Y. Matsuo, K. Tahara, Y. Sugie. Carbon, 35 (1997), pp. 113-120

[26] Y. Matsuo, K. Tahara, Y. Sugie. *Carbon*, 34 (1996), pp. 672-674

[27] Y. Matsuo, K. Hatase, Y. Sugie. *Chem Mater*, 10 (1998), pp. 2266-2269

[28] J. Xu, Y. Hu, L. Song, Q. Wang, W. Fan. *Mater Res Bull*, 36 (2001), pp. 1833-1836

[29] P.G. Liu, P. Xiao, M. Xiao, K.C. Gong. *Chin J Polym Sci*, 18 (2000), pp. 413-418

[30] J.W. Gilman, T. Kashiwaga, M. Nyden, J.E.T. Brown, C.L. Jackson, S. Lomakin, *et al..* S. Al-Malaika, A. Golovoy, C.A. Wilkie (Eds.), *Chemistry and technology of polymer additives*, Blackwell Scientific, Oxford (1999), pp. 249-265

[31] J.W. Gilman, T. Kashiwagi, E.P. Gianellis, E. Manias, S. Lomakin, J.D. Lichtenhan, *et al..* M. Le Bras, G. Camino, S. Bourbigot, R Delobel (Eds.), *Fire retardancy: the use of intumescence*, Royal Society of Chemistry, Cambridge (1998), pp. 203-221

[32] J. Zhang, C.A. Wilkie. *Polym Degrad Stab*, 83 (2004), p. 301

[33] S. Su, D.D. Jiang, C.A. Wilkie. *Polym Degrad Stab*, 83 (2004), p. 321

[34] S. Su, D.D. Jiang, C.A. Wilkie. *Polym Degrad Stab*, 83 (2004), p. 333

[35] Su S, Jiang DD, Wilkie CA. *Polym Adv Tech*, in press.

[36] Su S, Jiang DD, Wilkie CA. *J Vinyl Add Tech*, in press.

[37] A. Usuki, Y. Kojima, M. Kawasumi, A. Okada, Y. Fukushima, T. Kurauchi, *et al. J Mater Res*, 8 (1993), p. 1179